J. Math. Biol. (2013) 67:535–567
DOI 10.1007/s00285-012-0561-6

Mathematical Biology

Estimation of the diffusion rate and crossing probability for biased edge movement between two different types of habitat

**MingQing Xiao · John D. Reeve ·
Dashun Xu · James T. Cronin**

Received: 10 October 2011 / Revised: 8 June 2012 / Published online: 13 July 2012

Abstract One of the fundamental goals of ecology is to examine how dispersal affects the distribution and dynamics of insects across natural landscapes. These landscapes are frequently divided into patches of habitat embedded in a matrix of several non-habitat regions, and dispersal behavior could vary within each landscape element as well as the edges between elements. Reaction–diffusion models are a common way of modeling dispersal and species interactions in such landscapes, but to apply these models we also need methods of estimating the diffusion rate and any edge behavior parameters. In this paper, we present a method of estimating the diffusion rate using the mean occupancy time for a circular region. We also use mean occupancy time to estimate a parameter (the crossing probability) that governs one type of edge behavior often used in these models, a biased random walk. These new methods have some advantages over other methods of estimating these parameters, including reduced computational cost and ease of use in the field. They also provide a method of estimating the diffusion rate for a particular location in space, compared to existing

---

This research was supported by NSF DEB 0515781, 1021203 and DMS 0719783.

M. Xiao (✉) · D. Xu
Department of Mathematics, Southern Illinois University, Carbondale, IL 62901, USA
e-mail: mxiao@siu.edu

D. Xu
e-mail: dxu@math.siu.edu

J. D. Reeve
Department of Zoology, Southern Illinois University, Carbondale, IL 62901, USA
e-mail: jreeve@zoology.siu.edu

J. T. Cronin
Department of Biological Science, Louisiana State University, Baton Rouge, LA 70803, USA
e-mail: jcronin@lsu.edu

methods that represent averages over large areas. We further examine the statistical properties of the new method through simulation, and discuss how mean occupancy time could be estimated in field experiments.

Keywords Diffusion rate · Crossing probability · Edge behavior · Biased movement

Mathematics Subject Classification (2010) Primary 92B05 · 92D25; Secondary 92D40 · 92D50

1 Introduction

One of the fundamental goals of ecology is to determine how spatial complexity affects the distribution and dynamics of populations, as well as interactions among species. A number of studies clearly indicate that the movement and dispersal of insects may depend critically on the spatial arrangement and composition of landscape elements and the boundaries between them (Lawrence and Bach 1989; Roland et al. 2000; Ricketts 2001; Ries and Debinski 2001; Ovaskainen 2004). For example, the planthopper *Prokelisia crocea* inhabits a complex landscape composed of patches of its host plant cordgrass (*Spartina pectinata*) embedded in a matrix of mudflat, other native grasses, and the introduced grass smooth brome (*Bromus inermis*). Dispersal rates vary radically between these different landscape elements, and these insects also show differences in their movements for different boundary types. In particular, dispersal or diffusion rates for these insects are much higher on mudflat versus cordgrass or brome, and they rarely emigrate across a cordgrass–mudflat boundary but exhibit no such restraint for cordgrass–brome ones (Haynes and Cronin 2003, 2006; Reeve et al. 2008). These differences in dispersal behavior are also reflected in the population dynamics of this system. Patches of cordgrass surrounded by brome typically have lower and more variable planthopper densities and populations that are very extinction prone, relative to patches in mudflat (Cronin and Haynes 2004; Cronin 2007).

A common way to understand how such spatial complexity affects population dynamics is through reaction–diffusion models, because this mathematical framework can readily incorporate the movement of insects as well as species interactions (Kareiva and Odell 1987; Cantrell and Cosner 2003; Okubo and Levin 2001). However, it can be quite challenging to estimate the parameters for these models, especially for natural systems where the landscape is a mosaic of different elements. The different landscape elements could potentially have a different diffusion rates, dispersal behavior at edge or boundaries could vary with boundary type, and spatial differences in mortality and reproductive rates would also be expected. Estimates of all these parameters may be needed to realistically model the dynamics of populations inhabiting such landscapes.

A number of estimation methods for the dispersal parameters in reaction–diffusion models can be found in the literature. One method of estimating the diffusion rate is to release a large number of marked individuals at a point in space, whose position is then recorded over time across a grid of trapping or observation sites (Turchin 1998). A diffusion model is then fitted to these observations using least squares or maximum likelihood, resulting in an estimate of the diffusion coefficient. A variant of this approach involves the release of marked individuals at points in space in different habitat types as well as edges between types, then fitting models that incorporates different diffusion rates for each habitat type. Edge behavior can also be modeled as a biased random walk (Ovaskainen and Cornell 2003; Ovaskainen 2004; Reeve et al. 2008) or spatial differences in advection rates (Reeve and Cronin 2010). An alternative approach is the extended observation of the movements for individual insects, and fitting a diffusion model to the resulting series of locations and times (Cain 1990; Turchin 1998; Ovaskainen 2004). However, all these approaches require tracking the location of a large number of insects, and can be computationally intensive when the model equations are solved numerically. Another drawback of these methods is that their estimates of the diffusion rate are essentially averages over a large area. For example, Cronin et al. (2000) used a mark-recapture grid (square, 4 km on a side) to examine the movements of the clerid beetle *Thanasimus dubius*, a common predator of bark beetles. The diffusion rate might vary across space in this system, but this variation would be difficult to detect using these methods.

Fagan (1997) proposed a complement of existing methods for estimating the diffusion rate. The organisms are released within a square, and the cumulative proportion reaching the edge recorded over time. The solution of a diffusion model predicting this quantity is then fitted to the data using least squares, and an estimate of the diffusion rate so obtained. This method avoids the problem of tracking individual insects or observing their density on a grid, but does require that an absorbing barrier of traps completely surround the square. Moreover, the solution to be fitted is complex in form and extensive computation is required.

In this paper, we provide the mathematical means to estimate the diffusion rate, as well as the mortality rate during dispersal, using the mean occupancy time for insects released within a circular area. The rationale here is that mean occupancy time is a function of the diffusion and mortality rates, and given an estimate of mean occupancy time we should be able to solve for these parameters. Considering that many insects themselves are much smaller than the size of patch they reside in, the patch will usually be larger in scale than the distances between their movement steps. For example, one planthopper we have studied is under 1 cm in length and disperses by walking (or hopping), while the observed area in the experiments is on the order of 50–100 cm (Reeve et al. 2008). So, one would expect the diffusion approximation to hold in cases where the circular area is significantly larger than the step length. In any event, this assumption can be checked by comparing the cumulative distribution of occupancy times with the theoretical ones generated by the models.

We further use this method to obtain parameter estimates for one kind of edge behavior, a biased random walk (Ovaskainen 2004). This type of edge behavior is governed by a single parameter, the crossing probability for an insect on the boundary between two landscape elements. We show how this quantity can be estimated using the mean occupancy time for a circular patch of habitat surrounded by a matrix of non-habitat. We also examine the statistical properties of these estimation methods, including the amount of bias, the effect of sample size, and the performance of confidence intervals generated using the bootstrap percentile method. Although in this paper we choose a circular shape as the landscape element for the exposition of our approach, there is little restriction for the applications of the proposed method since many other type of areas can be transformed into a disk by means of various conformal mappings from the mathematical point of view (Sharon and Mumford 2007). Similar methods can also be applied to rectangular shapes (Min et al. 2012)

Our new method of estimation using mean occupancy time has a number of advantages over other methods. Existing methods generally require locating the animal precisely in space, either by following individual animals or sampling their spatial distribution in detail. Mean occupancy time is potentially easier to estimate in general, because we need only determine when an animal leaves (or dies in) an area. Another advantage of this method is that estimates of the diffusion rate can be obtained for a particular location in space, defined by a small circular region. This differs from existing methods that likely yield parameter estimates that are averages over large areas. We discuss how mean occupancy time might be estimated through experiments later in the paper.

The paper is organized as follows. Section 2 provides a brief description of our main findings and numerical examples of the estimation methods, for readers more interested in applying these techniques. Section 3 illustrates the probability density for a circular patch surrounded by matrix, for various strengths of edge behavior in the form of a biased random walk, and expressions derived for mean occupancy time under various scenarios. Some results on conditional probability density are also presented. In Sect. 4 we show how fundamental solutions to these diffusion systems can be obtained using Bessel functions, and expressions derived for mean occupancy time under various scenarios. Section 5 demonstrates some numerical examples in terms of the probability density for a circular patch surrounded by matrix, for various strengths of edge behavior in the form of a biased random walk. Section 6 examines the statistical properties of our estimation methods under several different scenarios. The paper ends in concluding remarks that summarize the advantages of the method and outlines possible methods of estimating mean occupancy time in the field.

2 Main results

2.1 Estimation of diffusion rate

The linear diffusion model used to quantify insect movements in a two dimensional (homogenous) field is given by

$$\frac{\partial u}{\partial t} = D\left(\frac{\partial^2 u}{\partial x^2} + \frac{\partial^2 u}{\partial y^2}\right) - c_0 u \tag{2.1}$$

where u is the probability density of the insects which is subjected to the boundary conditions and initial conditions, the parameter c_0 is the disappearance rate of the insects during the experiment. Disappearance can include mortality as well as dispersal not captured by the experiment.

One important characterization of diffusion of insects in an area is the *mean occupancy time* which measures the average time period that the insects stay until they leave the area or die. Given an area Ω, the mathematical description of the insect mean occupancy time T_Ω in Ω can be seen as follows. Let $u(x, y; t)$ be the insect probability density function for $(x, y) \in \Omega$ at time t, then the mean occupancy time for insects at the location (x, y) is given by

$$\int_0^\infty u(x, y; t)dt.$$

Thus the mean occupancy time over the entire Ω is given by

$$T_\Omega = \int_\Omega \left(\int_0^\infty u(x, y; t)dt \right) d\Omega, \tag{2.2}$$

provided that the insect initial probability distribution is known.

In field experiments, it is quite common to observe that in a given area, the shorter mean occupancy time the insects have, the higher diffusion rate is expected. Thus for a given homogeneous area Ω, one may expect that there should be a (mathematical) quantitative connection between the mean occupancy time T_Ω and the diffusion rate D. This motivates us to estimate the diffusion rate D by using the mean occupancy time.

We consider a circular patch $\Omega_a := \{(x, y) \in \mathbb{R}^2 : x^2+y^2 \leq a^2\}$ with radius $a > 0$, composed of only one type of habitat, and assume that the boundary $\partial\Omega_a := \{(x, y) \in \mathbb{R}^2 : x^2 + y^2 = a^2\}$ of Ω_a is absorbing. For the convenience of the approach, the initial distribution of the insects is set to be radically symmetric, that is, $u|_{t=0} = f(r)$ where $0 \leq r \leq a$. Throughout the paper, we denote by J_ν and Y_ν Bessel functions of the first and the second kind of order ν, respectively (for more details about Bessel functions, see, e.g, Pinsky 1998).

In the case $c_0 = 0$, we obtain an explicit solution for D given by

$$D = \frac{4\pi a^2}{T_{\Omega_a}} \sum_{n=1}^\infty \frac{\int_0^a r J_0\left(\frac{r}{a}\mu_n\right) f(r)dr}{\mu_n^3 J_1(\mu_n)}, \tag{2.3}$$

where $\mu_n, n = 1, 2, \ldots,$ are zeros of J_0, and T_{Ω_a} is the mean occupancy time of the insects staying in Ω_a.

Suppose that an individual insect is initially located at $r = 0$ and the mean occupancy time T_{Ω_a} for this individual is known. In this case $f(r) = \frac{\delta(r)}{2\pi}$, thus one has

$$D = \frac{2a^2}{T_{\Omega_a}} \sum_{n=1}^\infty \frac{1}{\mu_n^3 J_1(\mu_n)}.$$

If we truncate the series to the tenth term, we have

$$D \approx \frac{2a^2}{T_{\Omega_a}} \sum_{n=1}^{10} \frac{1}{\mu_n^3 J_1(\mu_n)} = 0.2498\ \frac{a^2}{T_{\Omega_a}}. \tag{2.4}$$

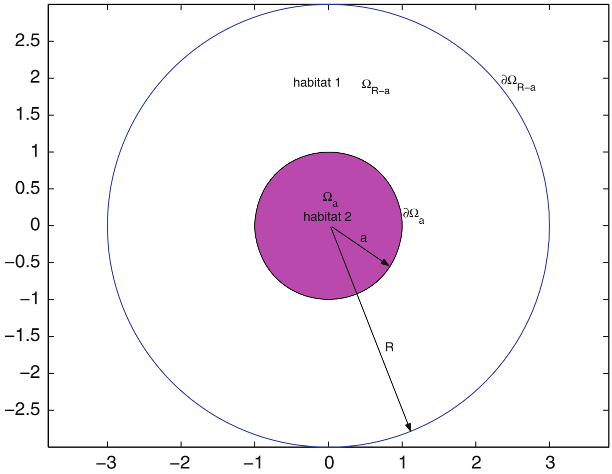

Fig. 1 A circular landscape with two different types of habitat

Here we pick terms up to the tenth since in this case one can show that the truncation error is the order of 10^{-4}, which is considered to meet the estimation requirement in general.

If c_0 also must be estimated, we need another mean occupancy time $T_{\Omega_b}, b \neq a$ with $u|_{t=0} = g(r)$. Then D and c_0 can be solved from the following two equations

$$\begin{aligned} T_{\Omega_a} &= 2\pi a^4 \sum_{n=1}^{\infty} \frac{\int_0^a r J_0\left(\frac{r}{a}\mu_n\right) f(r)dr}{\mu_n(c_0a^2 + D\mu_n^2)} \, J_1\left(\mu_n\right) \\ T_{\Omega_b} &= 2\pi b^4 \sum_{n=1}^{\infty} \frac{\int_0^b r J_0\left(\frac{r}{b}\mu_n\right) g(r)dr}{\mu_n(c_0b^2 + D\mu_n^2)} \, J_1\left(\mu_n\right). \end{aligned} \tag{2.5}$$

Section 6 will examine the statistical properties of the estimates obtained using (2.4) and (2.5).

2.2 Estimation of edge crossing probabilities

We consider two circular patch shapes with the same center. The inside circular disk Ω_a is composed of single type of habitat, such as a patch of host plants, which is surrounded by matrix or some other type of habitat Ω_{R-a} (see Fig. 1). The insects disperse away from a released location inside Ω_R. The behavior on the edge $\partial\Omega_a$ is modeled as a biased random walk (Ovaskainen and Cornell 2003; Ovaskainen 2004). In particular, a parameter k_1 describes the probability of an individual moving to Ω_a upon encountering the edge, while $k_2 = 1 - k_1$ is the probability of entering Ω_{R-a}. The edge condition implies a discontinuity in densities as one traverses the edge $\partial\Omega_a$ when $k_1 \neq k_2$. We further assume that there is no insect accumulation on the edge $\partial\Omega_a$, corresponding to general situation in reality. We denote by D_1 and D_2 the diffusion rates in Ω_a and Ω_{R-a}, respectively. The death rate in both habitats is assumed to be c_0. Then the diffusion model has the following mathematical representation:

$$\begin{aligned}
&\frac{\partial^2 u_1}{\partial r^2} + \frac{1}{r}\frac{\partial u_1}{\partial r} - \frac{c_0}{D_1}u_1 = \frac{1}{D_1}\frac{\partial u_1}{\partial t}, \quad 0 < r < a, t > 0,\\
&\frac{\partial^2 u_2}{\partial r^2} + \frac{1}{r}\frac{\partial u_2}{\partial r} - \frac{c_0}{D_2}u_2 = \frac{1}{D_2}\frac{\partial u_2}{\partial t}, \quad a < r < R, t > 0,\\
&u_1(r; 0) = f_1(r), \quad 0 \le r < a; \quad u_2(r; 0) = f_2(r), \quad a \le r \le R
\end{aligned} \tag{2.6}$$

subject to absorbing boundary condition:

$$u_2(R; t) = 0, \tag{2.7}$$

and edge conditions

$$\begin{aligned}
k_1 u_2(a + 0; t) &= k_2 u_1(a - 0; t),\\
D_1 \frac{\partial u_1}{\partial r}(a - 0; t) &= D_2 \frac{\partial u_2}{\partial r}(a + 0; t),
\end{aligned} \tag{2.8}$$

where $u_1(a - 0)$, $u_2(a + 0)$ stand for left-side and right-side limits, respectively, i.e.,

$$u_1(a - 0; t) := \lim_{r<a, r\to a} u_1(r; t), \quad u_2(a + 0; t) := \lim_{r>a, r\to a} u_2(r; t),$$

and we assume the initial condition function

$$f(r) = \begin{cases} f_1(r), & \text{if } 0 \le r < a \\ f_2(r), & \text{if } a < r \le R \end{cases}$$

is an integrable function on $0 \le r \le R$.

In the second part of the paper, we obtain the explicit mathematical expressions for the mean occupancy time T_{Ω_a} and $T_{\Omega_{R-a}}$ for circular regions Ω_a and Ω_{R-a}, respectively, in terms of the ratio $k = k_2/k_1$ where k_1 (resp. k_2) is the probability for insect to move in Ω_a (resp. Ω_{R-a}) upon encountering the boundary of Ω_a, assuming D_1 and D_2 estimated by the method presented in the Sect. 2.1. Here we denote two circular areas

$$\Omega_a = \left\{(x, y) \in \mathbb{R}^2 \ : \ x^2 + y^2 \le a\right\}, \quad \Omega_{R-a} = \left\{(x, y) \in \mathbb{R}^2 \ : \ a \le x^2 + y^2 \le R\right\}.$$

Next we compute the mean occupancy time T_{Ω_a} and $T_{\Omega_{R-a}}$ for a set of preselected k values by the results obtained in this paper. For example, in the case that an individual insect is initially located at $r = 0$, T_{Ω_a} and T_{Ω_R} for $k = k_2/k_1 = 1/9, 1/6, 1/3, 1, 3, 6, 9$ can be calculated below (see Table 1) by using (3.15) and (3.17). Observing that both T_{Ω_a} and $T_{\Omega_{R-a}}$ are monotonic (as expected), we then apply the piecewise cubic Hermite interpolation (PCHIP) to compute the unknown k's for a given T_{Ω_a} or $T_{\Omega_{R-a}}$. For example, suppose that we have obtained the mean occupancy

Table 1 Mean occupancy time for an individual located in the patch center initially

$a = 1, R = 3$	$k = 1/9$	$k = 1/6$	$k = 1/3$	$k = 1$	$k = 3$	$k = 6$	$k = 9$
T_{Ω_a}	1.7122	1.3334	0.8556	0.4607	0.3115	0.2724	0.2597
$T_{\Omega_{R-a}}$	0.4340	0.4847	0.5491	0.6035	0.6247	0.6306	0.6320

Table 2 Numerical estimation of crossing probability k_1 (i.e., the probability for insect to enter to Ω_a)

T_{Ω_a}	1.5950	1.1869	0.6672	0.3498	0.2922
Estimated value k_1^*	$k_1^* = 0.8913$	$k_1^* = 0.8333$	$k_1^* = 0.6602$	$k_1^* = 0.3187$	$k_1^* = 0.2004$
True value k_1	$k_1 = 0.8889$	$k_1 = 0.8333$	$k_1 = 0.6667$	$k_1 = 0.3333$	$k_1 = 0.2$
Error $\lvert k_1^* - k_1\rvert$	0.0024	0	0.0065	0.0146	0.0004

time $T_{\Omega_a} = 0.6672$ through an experiment. Then by applying PCHIP (matlab command 'inperp1') to the data given in Table 1, we obtain the estimate $k^* = 0.5146$, which yields the crossing probability $k_1^* = 0.2004$. In other words, the estimated probability for the insect to enter Ω_a is 0.2004 and thus the probability for entering Ω_{R-a} is $1 - 0.2004 = 0.7996$. The actual crossing probability $k_1 = 0.2$ since $T_{\Omega_a}(k_1 = 0.2) = 0.6672$ according to our obtained mathematical expression (3.15). We provide some numerical estimations in Table 2 for the purpose of comparisons. The estimation of k_2^* can be obtained by the relation $k_2^* = 1 - k_1^*$. The main outcomes in this paper help us to study how environmental heterogeneity affects an insect population. The computation of mean occupancy time in terms of crossing probability requires quite subtle analysis. The technical approach will be presented in the following sections.

3 Mean occupancy time in terms of conditional probability density

3.1 Homogeneous landscape

We consider here the case that insects are located inside a disk Ω_a of radius a on a homogeneous landscape. Assume that the insect initial distribution is independent of the polar angle, that is, $u(r; 0) = f(r)$. Then the mean occupancy time on the circumference of circle with radius $r < a$ is given by

$$2\pi r \int_0^\infty u(r; t)dt, \quad \text{for } 0 \le r \le a,$$

and the mean occupancy time in the disk centered at the origin with radius a can be obtained by

$$T_{\Omega_a} = 2\pi \int_0^a \int_0^\infty r u(r; t)dtdr.$$

We further assume that the boundary of Ω_a is absorbing.

Theorem 3.1 *Let* $u := u(x, y; t)$ *be the probability density function satisfying the two dimensional diffusion model* (2.1) *on* Ω_a *with absorbing boundary condition. The insect initial distribution is independent of the polar angle. Then the mean occupancy time for insects to be in* Ω_a *is given by*

$$T_{\Omega_a} = 2\pi a^4 \sum_{n=1}^{\infty} \frac{A_n J_1(\mu_n)}{\mu_n(c_0 a^2 + D\mu_n^2)},$$

where a *is the radius of the disk* Ω_a, μ_n *is the* nth*-zero of* J_0, *the Bessel functions of the first kind of order zero, and*

$$A_n = \frac{2\int_0^a rJ_0\left(\frac{r}{a}\mu_n\right) f(r)dr}{a^2 J_1(\mu_n)^2} \quad n = 1, 2, 3, \ldots,$$

in which f *is the insect initial distribution.*

Proof By using polar coordinates, the diffusion model (2.1) takes the form

$$\begin{aligned} &\frac{\partial^2 u}{\partial r^2} + \frac{1}{r}\frac{\partial u}{\partial r} - \frac{c_0}{D}u = \frac{1}{D}\frac{\partial u}{\partial t}, \quad 0 < r < a, t > 0, \\ &u(a;t) = 0, \quad t > 0, \\ &u(r;0) = f(r), \quad 0 \le r \le a. \end{aligned} \tag{3.9}$$

We will show later that the solution of (3.9) can be expressed in terms of the Bessel function J_0 of the first kind of order 0 as follows:

$$u(r;t) = \sum_{n=1}^{\infty} A_n J_0\left(\frac{r}{a}\mu_n\right) e^{-(c_0 + D\mu_n^2/a^2)t}, \tag{3.10}$$

where $\mu_n, n = 1, 2, \ldots,$ are zeros of J_0, and A_n is given by

$$A_n = \frac{\int_0^a rJ_0\left(\frac{r}{a}\mu_n\right) f(r)dr}{\int_0^a rJ_0\left(\frac{r}{a}\mu_n\right)^2 dr} = \frac{\int_0^a rJ_0\left(\frac{r}{a}\mu_n\right) f(r)dr}{\frac{a^2}{2} J_1(\mu_n)^2}.$$

Note that the mean occupancy time for the circumference of a circle with radius r is given by

$$2\pi r \int_0^{\infty} u(r;t)dt, \quad \text{for } 0 \le r \le a,$$

and the mean occupancy time in a disk centered at the origin with radius a can be obtained by

$$T_{\Omega_a} = 2\pi \int_0^a \int_0^\infty r u(r;t) dt dr.$$

According to the Bessel function properties, one has

$$\int_0^a r J_0\left(\frac{r}{a}\mu_n\right) dr = \frac{a^2}{\mu_n} J_1(\mu_n),$$

and thus we have

$$\begin{aligned} T_{\Omega_a} &= 2\pi \int_0^a \int_0^\infty r u(r;t) dt dr = 2\pi a^2 \sum_{n=1}^{\infty} \frac{A_n}{(c_0 a^2 + D\mu_n^2)} \int_0^a r J_0\left(\frac{r}{a}\mu_n\right) dr \\ &= 2\pi a^4 \sum_{n=1}^{\infty} \frac{A_n}{\mu_n (c_0 a^2 + D\mu_n^2)} J_1(\mu_n), \end{aligned}$$

which gives the expression of the insect mean occupancy time in Ω_a.

In general, in order to obtain c_0 and D, we need another mean occupancy time T_{Ω_b} with $b \neq a$. Usually, we may be able to choose a small radius a so that the disappearance rate $c_0 = 0$ inside Ω_a. In such a case, one can have

$$D = \frac{2\pi a^4}{T_{\Omega_a}} \sum_{n=1}^{\infty} \frac{A_n}{\mu_n^3} J_1(\mu_n).$$

Suppose that an individual insect is located at $r = 0$ and the mean occupancy time T_{Ω_a} is known. Note that in this case $f(r) = \frac{\delta(r)}{2\pi}$ and

$$A_n = \frac{\int_0^a r J_0\left(\frac{r}{a}\mu_n\right) f(r) dr}{\frac{a^2}{2} J_1(\mu_n)^2} = \frac{1}{\pi a^2 J_1(\mu_n)^2}$$

thus we have

$$D = \frac{2a^2}{T_{\Omega_a}} \sum_{n=1}^{\infty} \frac{1}{\mu_n^3 J_1(\mu_n)}.$$

Recall that $\{\mu_n\}$ is a set of zeros of J_0, which is known. Hence the diffusion rate D can be approximated to an arbitrary given accuracy. We here list the first ten μ_n's,

$$\begin{aligned} &\mu_1 = 2.405, \mu_2 = 5.520, \mu_3 = 8.654, \mu_4 = 11.792, \mu_5 = 14.931 \\ &\mu_6 = 18.071, \mu_7 = 21.212, \mu_8 = 24.352, \mu_9 = 27.493, \mu_{10} = 30.635. \end{aligned}$$

Using these ten terms we have

$$D \approx \frac{2a^2}{T_{\Omega_a}} \sum_{n=1}^{10} \frac{1}{\mu_n^3 J_1(\mu_n)} = 0.2498 \, \frac{a^2}{T_{\Omega_a}}$$

3.2 Non-homogeneous landscapes

As in the previous section, we denote by Ω_a the circular area of radius a, that is,

$$\Omega_a = \left\{ (x, y) : \text{ where } x^2 + y^2 \leq a \right\}.$$

We also denote by Ω_{R-a} the annual area between Ω_a and Ω_R with $a < R$, that is,

$$\Omega_{R-a} = \left\{ (x, y) : \text{ where } a \leq x^2 + y^2 \leq R \right\}.$$

Now we assume that Ω_a is one type of habitat, while Ω_{R-a} is another type of habitat. We assume that insects' initial distribution is radically symmetric. Let's consider the following diffusion equation:

$$\begin{aligned} D_1 \left(\frac{\partial^2 u_1}{\partial r^2} + \frac{1}{r} \frac{\partial u_1}{\partial r} \right) - c_0 u_1 = \frac{\partial u_1}{\partial t}, \quad r^2 = x^2 + y^2, \ (x, y) \in \Omega_a, \ t > 0, \\ D_2 \left(\frac{\partial^2 u_2}{\partial r^2} + \frac{1}{r} \frac{\partial u_2}{\partial r} \right) - c_0 u_2 = \frac{\partial u_2}{\partial t}, \quad r^2 = x^2 + y^2, \ (x, y) \in \Omega_{R-a}, \ t > 0. \end{aligned} \tag{3.11}$$

subject to absorbing boundary condition:

$$u_2(R; t) = 0, \tag{3.12}$$

and edge conditions

$$\begin{aligned} k_1 u_2(a + 0; t) = k_2 u_1(a - 0; t), \\ D_1 \frac{\partial u_1}{\partial r}(a - 0; t) = D_2 \frac{\partial u_2}{\partial r}(a + 0; t). \end{aligned} \tag{3.13}$$

In next section, we will show the following theorem which is a direct result of Theorem 4.4.

Theorem 3.2 *The probability density before the insect will hit $\partial\Omega_a$ or die at time t is given by*

$$u_1(r; t) = \sum_{n=1}^{\infty} \frac{A_n z_{\lambda_n}(a)}{y_{\lambda_n}(a)} J_0\left(r \sqrt{\frac{\lambda_n}{D_1}} \right) \quad \textit{for } 0 \leq r < a;$$

and the probability density that the insect will hit $\partial\Omega_a$ before it hit $\partial\Omega_R$ or die at the time t is given by

$$u_2(r;t) = \sum_{n=1}^{\infty} kA_n z_{\lambda_n}(r) e^{-(c_0+\lambda_n)t} \quad \textit{for } a < r < R;$$

where y_{λ_n} and z_{λ_n} are given by

$$\begin{aligned} y_{\lambda_n}(r) &= J_0\left(r\sqrt{\tfrac{\lambda_n}{D_1}}\right) \\ z_{\lambda_n}(r) &= J_0\left(r\sqrt{\tfrac{\lambda_n}{D_2}}\right) Y_0\left(R\sqrt{\tfrac{\lambda_n}{D_2}}\right) - J_0\left(R\sqrt{\tfrac{\lambda_n}{D_2}}\right) Y_0\left(r\sqrt{\tfrac{\lambda_n}{D_2}}\right), \end{aligned} \tag{3.14}$$

and λ_n is determined by (4.28).

Now we are ready to state the following result:

Theorem 3.3 *Suppose that in Ω_R insect initial distribution satisfies*

$$f(r) = \begin{cases} f_1(r), & \textit{if } 0 \le r < a \\ f_2(r), & \textit{if } a < r \le R \end{cases}$$

which is an integrable function on $0 \le r \le R$. Then the mean occupancy time for insects to be in Ω_a is

$$T_{\Omega_a} = 2\pi a\sqrt{D_1} \sum_{n=1}^{\infty} \frac{A_n z_{\lambda_n}(a)}{\sqrt{\lambda_n}(c_0+\lambda_n) y_{\lambda_n}(a)} \, J_1\left(a\sqrt{\frac{\lambda_n}{D_1}}\right) \tag{3.15}$$

where y_{λ_n}, z_{λ_n} are defined by (3.14), and A_n satisfies

$$\begin{aligned} &\int_0^a f_1(r) r w_{\lambda_n}(r)dr + \frac{1}{k}\int_a^R f_2(r) r w_{\lambda_n}(r)dr \\ &\quad = A_n\left(\int_0^a r w_{\lambda_n}^2(r)dr + \frac{1}{k}\int_a^R r w_{\lambda_n}^2(r)dr\right). \end{aligned} \tag{3.16}$$

Proof According to theorem 4.4 of next section, the solution of (3.11)–(3.13) on Ω_a is given by

$$u(r;t) = \sum_{n=1}^{\infty} A_n \frac{z_{\lambda_n}(a)}{y_{\lambda_n}(a)} J_0\left(r\sqrt{\frac{\lambda_n}{D_1}}\right) e^{-(c_0+\lambda_n)},$$

where A_n satisfies (3.16). From the property of Bessel function, we know that $(d/dr)(rJ_1) = (rJ_0)$, and we thus have

$$\int_0^a rJ_0\left(r\sqrt{\frac{\lambda_n}{D_1}}\right)dr = a\sqrt{\frac{D_1}{\lambda_n}}\, J_1\left(a\sqrt{\frac{\lambda_n}{D_1}}\right).$$

Now we can calculate the mean occupancy time as follows:

$$\begin{aligned} T_{\Omega_a} &= 2\pi\int_0^a\int_0^\infty ru(r;t)dtdr = 2\pi\sum_{n=1}^\infty \frac{A_n z_{\lambda_n}(a)}{(c_0+\lambda_n)y_{\lambda_n}(a)}\int_0^a y_{\lambda_n}(r)dr \\ &= 2\pi\sum_{n=1}^\infty \frac{A_n z_{\lambda_n}(a)}{(c_0+\lambda_n)y_{\lambda_n}(a)}\int_0^a rJ_0\left(r\sqrt{\frac{\lambda_n}{D_1}}\right)dr \\ &= 2\pi\sum_{n=1}^\infty \frac{aA_n\sqrt{D_1}z_{\lambda_n}(a)}{\sqrt{\lambda_n}(c_0+\lambda_n)y_{\lambda_n}(a)}\, J_1\left(a\sqrt{\frac{\lambda_n}{D_1}}\right) \end{aligned}$$

which yields the result.

Corollary 3.4 *Suppose that an individual insect is located at $r = 0$ initially. Then the mean occupancy time in Ω_a is given by*

$$T_{\Omega_a} = a\sqrt{D_1}\sum_{n=1}^\infty \frac{z^2_{\lambda_n}(a)}{\Delta_n\sqrt{\lambda_n}(c_0+\lambda_n)y^2_{\lambda_n}(a)}\, J_1\left(a\sqrt{\frac{\lambda_n}{D_1}}\right),$$

where Δ_n is given by (4.37).

Similarly, for the domain Ω_{R-a}, we have

Theorem 3.5 *Under the assumption of Theorem 3.3, the mean occupancy time for insects to be in Ω_{R-a} is*

$$T_{\Omega_{R-a}} = 2\pi k\sqrt{D_2}\sum_{n=1}^\infty \frac{A_n}{\sqrt{\lambda_n}(c_0+\lambda_n)}\begin{vmatrix} 0 & J_0\left(R\sqrt{\frac{\lambda_n}{D_2}}\right) & Y_0\left(R\sqrt{\frac{\lambda_n}{D_2}}\right) \\ R & J_1\left(a\sqrt{\frac{\lambda_n}{D_2}}\right) & Y_1\left(a\sqrt{\frac{\lambda_n}{D_2}}\right) \\ a & J_1\left(R\sqrt{\frac{\lambda_n}{D_2}}\right) & Y_1\left(R\sqrt{\frac{\lambda_n}{D_2}}\right) \end{vmatrix} \tag{3.17}$$

where z_{λ_n} is defined by (3.14).

Proof Again according to Theorem 4.4, the solution of (3.11)–(3.13) on Ω_{R-a} has a form:

$$u(r;t) = \sum_{n=1}^\infty kA_n z_{\lambda_n}(r)J_0\left(r\sqrt{\frac{\lambda_n}{D_1}}\right)e^{-(c_0+\lambda_n)},$$

By applying the properties of Bessel function $(d/dr)(rJ_1) = (rJ_0)$ and $(d/dr)(rY_1) = (rY_0)$, we have

$$\int_a^R rJ_0\left(r\sqrt{\frac{\lambda_n}{D_2}}\right)dr = \sqrt{\frac{D_2}{\lambda_n}}\left(RJ_1\left(R\sqrt{\frac{\lambda_n}{D_2}}\right) - aJ_1\left(a\sqrt{\frac{\lambda_n}{D_2}}\right)\right) \tag{3.18}$$

and

$$\int_a^R rY_0\left(r\sqrt{\frac{\lambda_n}{D_2}}\right)dr = \sqrt{\frac{D_2}{\lambda_n}}\left(RY_1\left(R\sqrt{\frac{\lambda_n}{D_2}}\right) - aY_1\left(a\sqrt{\frac{\lambda_n}{D_2}}\right)\right). \tag{3.19}$$

Therefore, the mean occupancy time for insects to be in Ω_{R-a} is

$$\begin{aligned} T_{\Omega_{R-a}} &= 2\pi \int_a^R \int_0^\infty ru(r;t)dtdr = 2\pi \sum_{n=1}^\infty \frac{kA_n}{c_0+\lambda_n} \int_a^R rz_{\lambda_n}(r)dr, \\ &= 2\pi \sum_{n=1}^\infty \frac{kA_n}{c_0+\lambda_n}\left(\int_a^R rJ_0\left(r\sqrt{\frac{\lambda_n}{D_2}}\right)dr\ Y_0\left(R\sqrt{\frac{\lambda_n}{D_2}}\right)\right. \\ &\quad \left. - J_0\left(R\sqrt{\frac{\lambda_n}{D_2}}\right)\int_a^R rY_0\left(r\sqrt{\frac{\lambda_n}{D_2}}\right)dr\right). \end{aligned}$$

Applying (3.18) and (3.19) leads to the desired result.

Corollary 3.6 *Suppose that an individual insect is located at* $r = 0$ *initially. Then the mean occupancy time in* Ω_{R-a} *is given by*

$$T_{\Omega_{R-a}} = k\sqrt{D_2}\sum_{n=1}^\infty \frac{1}{\Delta_n\sqrt{\lambda_n}(c_0+\lambda_n)}\begin{vmatrix} 0 & J_0\left(R\sqrt{\frac{\lambda_n}{D_2}}\right) & Y_0\left(R\sqrt{\frac{\lambda_n}{D_2}}\right) \\ R & J_1\left(a\sqrt{\frac{\lambda_n}{D_2}}\right) & Y_1\left(a\sqrt{\frac{\lambda_n}{D_2}}\right) \\ a & J_1\left(R\sqrt{\frac{\lambda_n}{D_2}}\right) & Y_1\left(R\sqrt{\frac{\lambda_n}{D_2}}\right) \end{vmatrix},$$

where Δ_n *is given by* (4.37).

4 Probability density functions

In this section we are going to develop the expressions of probability density functions used in previous sections. Again recall that throughout the paper, we denote by J_ν and Y_ν the Bessel functions of the first and the second kind of order ν, respectively.

We first solve the diffusion equation (3.9) to get the probability density function u. The approach for this case is to seek a separated solution in the form of

$$u(r;t) = R(r)T(t).$$

Substituting into (3.9), we have

$$\frac{T'(t) + c_0 T(t)}{DT(t)} = \frac{R''(r) + (1/r)R'(r)}{R(r)}.$$

Hence, each side equals to the same constant, which we denote $-\nu$. Then we arrive at the following two differential equations:

$$\begin{gathered} T'(t) + (c_0 + D\mu)T(t) = 0 \\ R''(r) + (1/r)R'(r) + \mu R(r) = 0. \end{gathered}$$

The solution must be finite at $r = 0$, so the required separated solutions are $J_0(r\sqrt{\nu})e^{-(c_0+D\nu t)}$. The boundary condition of (3.9) $u(a;t) = 0$ requires $J_0(a\sqrt{\nu}) = 0$; thus $r\sqrt{\nu} = \mu_n$, a positive zero of the Bessel function J_0. The solution takes the form

$$u(r;t) = \sum_{n=1}^{\infty} A_n J_0\left(\frac{r}{a}\mu_n\right) e^{-(c_0+D\mu_n^2/a^2)t}$$

where A_n is determined by the initial distribution.

Next we will find the probability density function on a nonhomogeneous landscape Ω_R. This case is much more complicated and we will present the solution in terms of a sequence of lemmas and theorems. For the convenience of later discussion, we denote $k = k_2/k_1$. To begin, we look for separations of the diffusion equations

$$\frac{\partial^2 \bar{u}_i}{\partial r^2} + \frac{1}{r}\frac{\partial \bar{u}_i}{\partial r} = \frac{1}{D_i}\frac{\partial \bar{u}_i}{\partial t}, \tag{4.20}$$

where $i = 1, 2$. We let $\bar{u}_i(r;t) = R_i(r)T_i(t)$ and substitute it into the equations. We obtain

$$\frac{T_i'(t)}{T_i(t)} = D_i \frac{R_i'' + (1/rR_i')}{R_i}.$$

The right side depends on r, whereas the left side depends on t. Therefore each is a constant, which we call $-\lambda$ for both $i = 1$ and $i = 2$. Thus

$$T_i'(t) + \lambda T_i(t) = 0, \tag{4.21}$$

and

$$R_i'' + \tfrac{1}{r} R_i' + \tfrac{\lambda}{D_i} R_i = 0. \tag{4.22}$$

Equation (4.22) is a Bessel's equation with angular index $\nu = 0$. Its general solution is given by

$$R_i(r) = A_i J_0\left(r\sqrt{\frac{\lambda}{D_i}}\right) + B_i Y_0\left(r\sqrt{\frac{\lambda}{D_i}}\right)$$

where A_i and B_i are arbitrary constants. Therefore, a solution of (4.20) has a form of

$$\bar{u}_i(r;t) = \left(A_i J_0\left(r\sqrt{\frac{\lambda}{D_i}}\right) + B_i Y_0\left(r\sqrt{\frac{\lambda}{D_i}}\right)\right) e^{-\lambda t}. \tag{4.23}$$

It is easy to see that the relationship between $\bar{u}_i$ and the solution u_i of

$$\frac{\partial^2 u_i}{\partial r^2} + \frac{1}{r}\frac{\partial u_i}{\partial r} - c_0 u_i = \frac{1}{D_i}\frac{\partial u_i}{\partial t}$$

is given by

$$u_i(r;t) = e^{-c_0 t}\bar{u}_i(r;t). \tag{4.24}$$

Thus we have

$$u_i(r;t) = \left(A_i J_0\left(r\sqrt{\frac{\lambda}{D_i}}\right) + B_i Y_0\left(r\sqrt{\frac{\lambda}{D_i}}\right)\right) e^{-(c_0+\lambda)t}.$$

Next we apply the boundary condition (2.7) and edge condition (2.8) to above solution for $i = 1, 2$ respectively. Note when $i = 1$, the solution u_1 should be well-defined in the disk $0 \le r < a$, while $r = 0$ is a singular point for Y_0. Hence we have $B_1 = 0$. Thus

$$u_1(r;t) = A_1 J_0\left(r\sqrt{\frac{\lambda}{D_1}}\right) e^{-(c_0+\lambda)t}. \tag{4.25}$$

When $i = 2$, by noticing $u_2(R;t) = 0$, the solution u_2 can be written as

$$u_2(r;t) = \bar{C}\Big(J_0\left(r\sqrt{\tfrac{\lambda}{D_2}}\right) Y_0\left(R\sqrt{\tfrac{\lambda}{D_2}}\right) - J_0\left(R\sqrt{\tfrac{\lambda}{D_2}}\right) Y_0\left(r\sqrt{\tfrac{\lambda}{D_2}}\right)\Big) e^{-(c_0+\lambda)t}, \tag{4.26}$$

where $\bar{C}$ is an arbitrary constant. Now by applying edge condition (2.8), we have

$$\begin{aligned}
&kA_1 J_0\left(a\sqrt{\frac{\lambda}{D_1}}\right) = \bar{C}\left(J_0\left(a\sqrt{\frac{\lambda}{D_2}}\right)Y_0\left(R\sqrt{\frac{\lambda}{D_2}}\right)\right.\\
&\quad\left. - J_0\left(R\sqrt{\frac{\lambda}{D_2}}\right)Y_0\left(a\sqrt{\frac{\lambda}{D_2}}\right)\right) - A_1\sqrt{D_1\lambda}J_1\left(a\sqrt{\frac{\lambda}{D_1}}\right)\\
&\quad = \bar{C}\sqrt{D_2\lambda}\left(-J_1\left(a\sqrt{\frac{\lambda}{D_2}}\right)Y_0\left(R\sqrt{\frac{\lambda}{D_2}}\right) - J_0\left(R\sqrt{\frac{\lambda}{D_2}}\right)Y_0'\left(a\sqrt{\frac{\lambda}{D_2}}\right)\right).
\end{aligned} \tag{4.27}$$

These two algebraic equations yield a simultaneous homogeneous linear system for A_1 and $\bar{C}$. As we require a nonzero solution, the determinant of the coefficients must vanish. This gives

$$\begin{aligned}
&k\sqrt{\lambda D_2}J_0\left(a\sqrt{\frac{\lambda}{D_1}}\right)\left(J_1\left(a\sqrt{\frac{\lambda}{D_2}}\right)Y_0\left(R\sqrt{\frac{\lambda}{D_2}}\right) - J_0\left(R\sqrt{\frac{\lambda}{D_2}}\right)Y_1\left(a\sqrt{\frac{\lambda}{D_2}}\right)\right)\\
&= \sqrt{\lambda D_1}J_1\left(a\sqrt{\frac{\lambda}{D_1}}\right)\left(J_0\left(a\sqrt{\frac{\lambda}{D_2}}\right)Y_0\left(R\sqrt{\frac{\lambda}{D_2}}\right)\right.\\
&\quad\left. - J_0\left(R\sqrt{\frac{\lambda}{D_2}}\right)Y_0\left(a\sqrt{\frac{\lambda}{D_2}}\right)\right)
\end{aligned} \tag{4.28}$$

by applying $Y_0'(x) = -Y_1(x)$. We denote by $g_1(\lambda)$ the left-handed side function of (4.28) and by $g_2(\lambda)$ the right handed side function. Then the solution λ of (4.28) is given by $g_1(\lambda) = g_2(\lambda)$ (see Fig. 2).

We list the first five solutions of (4.28) corresponding $k_2/k_1 = 1/9$, $1/3$, $1/6$, 1, 3, 6, 9 in Table 3. From the table, one can see that the principle eigenvalue λ_1 increases as k increases. This, in turn, implies that insect population in Ω_R decreases faster as k increases.

Let us denote $\{\lambda_n\}_{n=1}^{\infty}$ the positive solution of the above equation. According to classical theory, u_1 can be expressed by Fourier–Bessel expression:

$$u_1(r;t) = \sum_{n=1}^{\infty} A_n J_0\left(r\sqrt{\frac{\lambda_n}{D_1}}\right)e^{-(c_0+\lambda_n)t} \tag{4.29}$$

for $0 \le r < a$. Note initial condition $u_1(r;0) = f(r)$, we then have

$$\frac{1}{2}\left[f(r+0) + f(r-0)\right] = \sum_{n=1}^{\infty} A_n J_0\left(r\sqrt{\frac{\lambda_n}{D_1}}\right).$$

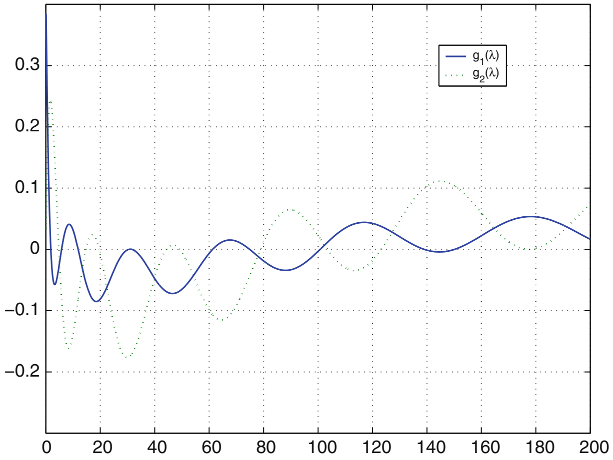

Fig. 2 Plots g_1 and g_2 with $D_1 = 1$, $D_2 = 2$, $k_1 = 0.75$, $k_2 = 0.25$, $a = 1$, $R = 3$

Table 3 The first five solutions of (4.28) corresponding to different k's

$k = k_2/k_1$	λ_1	λ_2	λ_3	λ_4	λ_5
1/9	0.3349	4.8923	14.0503	20.8472	41.9914
1/6	0.4621	4.9344	13.8455	21.3192	41.3256
1/3	0.7440	5.0410	13.4279	22.3973	39.9581
1	1.2446	5.2928	12.7410	24.6328	37.4814
3	1.5924	5.5421	12.2568	26.8464	35.2369
6	1.7089	5.6466	12.0851	27.9491	34.1461
9	1.7512	5.6880	12.0209	28.4684	33.6340

Unfortunately, the set of functions $\{J_0(r\sqrt{\frac{\lambda_n}{D_1}})\}_{n=1}^{\infty}$, where the eigenvalues $\{\lambda_n\}_{n=1}^{\infty}$ are obtained from (4.28), is not orthogonal in $L^2(0, a)$. Thus in order to solve the problem, we have to look for a set of orthogonal functions. Let us denote

$$y_\lambda(r) = J_0\left(r\sqrt{\frac{\lambda}{D_1}}\right) \tag{4.30}$$

$$z_\lambda(r) = J_0\left(r\sqrt{\frac{\lambda}{D_2}}\right)Y_0\left(R\sqrt{\frac{\lambda}{D_2}}\right) - J_0\left(R\sqrt{\frac{\lambda}{D_2}}\right)Y_0\left(r\sqrt{\frac{\lambda}{D_2}}\right),$$

and define a function w in $[0, R]$ as

$$w_\lambda(r) = \begin{cases} \dfrac{z_\lambda(a)}{y_\lambda(a)}\, y_\lambda(r), & \text{if } \ 0 \le r < a \\[2ex] k\, z_\lambda(r), & \text{if } \ a \le r \le R \end{cases} \tag{4.31}$$

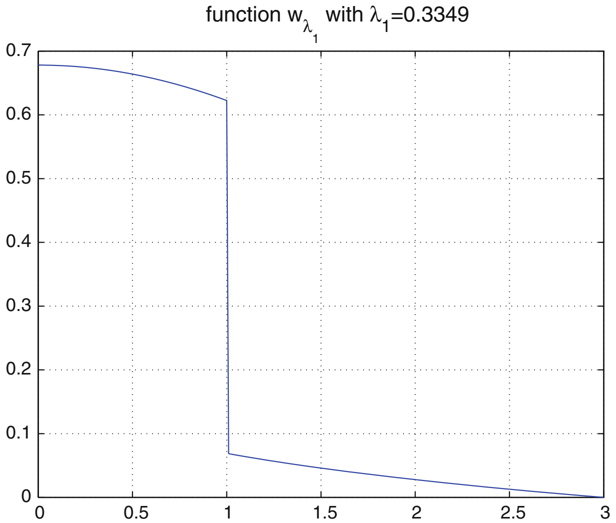

Fig. 3 w_{λ_1} function with $D_1 = 1$, $D_2 = 2$, $k_1 = 0.9$, $k_2 = 0.1$, $a = 1$, $R = 3$

The motivation for introducing w is given by following lemmas (Fig. 3).

Lemma 4.1 *The function $u(r;t) := w_\lambda(r)e^{-(c_0+\lambda)t}$ satisfies the diffusion equations appeared in (2.6) as well as the edge condition (2.8) and boundary condition (2.7).*

Proof It is straightforward to see that $u(r;t)$ satisfies both diffusion equations appeared in (2.6) as well as the boundary condition (2.7). We now verify that $u(r;t)$ also satisfies the edge condition (2.8). Notice that

$$u(a-0;t) = \lim_{r\to a-0} w_\lambda(r)e^{-(c_0+\lambda)t} = \frac{z_\lambda(a)}{y_\lambda(a)} y_\lambda(a)e^{-(c_0+\lambda)t} = z_\lambda(a)e^{-(c_0+\lambda)t}$$

and

$$u(a+0;t) = \lim_{r\to a-0} w_\lambda(r)e^{-(c_0+\lambda)t} = k\ z_\lambda(a)e^{-(c_0+\lambda)t}.$$

Thus $u(a+0;t) = ku(a-0;t)$. This verifies the first edge condition. For the second edge condition, one can see

$$D_1\frac{\partial u_1}{\partial r}(a-0;t) = D_1\frac{z_\lambda(a)}{y_\lambda(a)} y'_\lambda(a)e^{-(c_0+\lambda)t}$$

and

$$D_2\frac{\partial u_2}{\partial r}(a+0;t) = D_2 k\ z'_\lambda(a)e^{-(c_0+\lambda)t}.$$

The choice of λ obtained from (4.28) leads to

$$D_1 \frac{z_\lambda(a)}{y_\lambda(a)} y'_\lambda(a) = D_2 k\ z'_\lambda(a).$$

Hence the proof is complete.

We denote by $L^2_{a,k}(0, R)$ the space which consists of all square integrable functions in $(0, R)$ with an inner product

$$\langle \cdot, \cdot \rangle := \langle \cdot, \cdot \rangle_{L^2(0,a)} + \frac{1}{k} \langle \cdot, \cdot \rangle_{L2(a,R)}.$$

Lemma 4.2 *Let $\{\lambda_n\}_{n=1}^\infty$ be a sequence obtained from (4.28). Then the set of function $\{\sqrt{r}\ w_{\lambda_n}(r)\}_{n=1}^\infty$ is orthogonal in $L^2_{a,k}(0, R)$.*

Proof Notice that $w_{\lambda_n}(r)$ satisfies the Bessel equations

$$\begin{array}{ll} (rw'_{\lambda_n}(r))' + \frac{r\lambda_n}{D_1} w_{\lambda_n}(r) = 0, & 0 \le r < a \\ (rw'_{\lambda_n}(r))' + \frac{r\lambda_n}{D_2} w_{\lambda_n}(r) = 0, & a \le r < R. \end{array} \tag{4.32}$$

Taking $\lambda_n = \lambda_{n_1}$ and multiplying by $w_{\lambda_{n_2}}$, we obtain, after integration by parts,

$$aw'_{\lambda_{n_1}}(a-0) w_{\lambda_{n_2}}(a-0) - \int_0^a r w'_{\lambda_{n_1}} w'_{\lambda_{n_2}} dr + \frac{\lambda_{n_1}}{D_1} \int_0^a w_{\lambda_{n_1}}(r) w_{\lambda_{n_2}}(r) dr$$

$$= 0 \quad \text{for } 0 \le r < a - aw'_{\lambda_{n_1}}(a+0) w_{\lambda_{n_2}}(a+0) - \int_a^R r w'_{\lambda_{n_1}}(r) w'_{\lambda_{n_2}}(r) dr$$

$$+ \frac{\lambda_{n_1}}{D_2} \int_a^R w_{\lambda_{n_1}}(r) w_{\lambda_{n_2}}(r) dr = 0 \quad \text{for } a \le r < R.$$

Interchanging the roles of $w_{\lambda_{n_1}}$ and $w_{\lambda_{n_2}}$ and subtracting the resulting equations lead to

$$\begin{aligned} & a\left(w'_{\lambda_{n_1}} w_{\lambda_{n_2}} - w'_{\lambda_{n_2}} w_{\lambda_{n_1}}\right)\Big|_{r=a-0} + \frac{\lambda_{n_1} - \lambda_{n_2}}{D_1} \int_0^a r w_{\lambda_{n_1}}(r) w_{\lambda_{n_2}}(r) dr = 0, \\ & \quad 0 \le r < a \\ & -a\left(w'_{\lambda_{n_1}} w_{\lambda_{n_2}} - w'_{\lambda_{n_2}} w_{\lambda_{n_1}}\right)\Big|_{r=a+0} + \frac{\lambda_{n_1} - \lambda_{n_2}}{D_2} \int_a^R r w_{\lambda_{n_1}}(r) w_{\lambda_{n_2}}(r) dr = 0, \\ & \quad a \le r < R. \end{aligned} \tag{4.33}$$

We next claim

$$D_1\left(w'_{\lambda_{n_1}}w_{\lambda_{n_2}}-w'_{\lambda_{n_2}}w_{\lambda_{n_1}}\right)\Big|_{r=a-0}=\frac{1}{k}D_2\left(w'_{\lambda_{n_1}}w_{\lambda_{n_2}}-w'_{\lambda_{n_2}}w_{\lambda_{n_1}}\right)\Big|_{r=a+0}$$

According to (4.31), we have

$$\begin{aligned}\left(w'_{\lambda_{n_1}}w_{\lambda_{n_2}}-w'_{\lambda_{n_2}}w_{\lambda_{n_1}}\right)\Big|_{r=a-0}&=\frac{z_{\lambda_{n_1}}(a)z_{\lambda_{n_2}}(a)}{y_{\lambda_{n_1}}(a)y_{\lambda_{n_2}}(a)}\left(y'_{\lambda_{n_1}}(a)y_{\lambda_{n_2}}(a)-y_{\lambda_{n_1}}(a)y'_{\lambda_{n_2}}(a)\right)\\&=z_{\lambda_{n_1}}(a)z_{\lambda_{n_2}}(a)\left(\frac{y'_{\lambda_{n_1}}(a)}{y_{\lambda_{n_1}}(a)}-\frac{y'_{\lambda_{n_2}}(a)}{y_{\lambda_{n_2}}(a)}\right).\end{aligned}$$

Edge condition (2.8) implies

$$\begin{aligned}\frac{y'_{\lambda_{n_1}}(a)}{y_{\lambda_{n_1}}(a)}&=k\frac{D_2}{D_1}\frac{z'_{\lambda_{n_1}}(a)}{z_{\lambda_{n_1}}(a)}\\\frac{y'_{\lambda_{n_2}}(a)}{y_{\lambda_{n_2}}(a)}&=k\frac{D_2}{D_1}\frac{z'_{\lambda_{n_2}}(a)}{z_{\lambda_{n_2}}(a)}.\end{aligned}$$

Hence we have

$$\begin{aligned}D_1\left(w'_{\lambda_{n_1}}w_{\lambda_{n_2}}-w'_{\lambda_{n_2}}w_{\lambda_{n_1}}\right)\Big|_{r=a-0}&=kD_2\left(z'_{\lambda_{n_1}}(a)z_{\lambda_{n_2}}(a)-z_{\lambda_{n_1}}(a)z'_{\lambda_{n_2}}(a)\right)\\&=\frac{1}{k}D_2\left(w'_{\lambda_{n_1}}w_{\lambda_{n_2}}-w'_{\lambda_{n_2}}w_{\lambda_{n_1}}\right)\Big|_{r=a+0}.\end{aligned}$$

Adding two equations in (4.33), we are ready to see

$$\int_0^a rw_{\lambda_{n_1}}(r)w_{\lambda_{n_2}}(r)dr+\frac{1}{k}\int_a^R rw_{\lambda_{n_1}}(r)w_{\lambda_{n_2}}(r)dr=0$$

since $\lambda_{n_1}\neq\lambda_{n_2}$. We thus complete the proof.

Lemma 4.3 *Let* $\{\lambda_n\}_{n=1}^{\infty}$ *be a sequence obtained from* (4.28). *Then*

$$\begin{aligned}\int_0^a rw^2_{\lambda_n}(r)dr+\frac{1}{k}\int_a^R rw^2_{\lambda_n}(r)dr&=\frac{1}{2}a^2(1-k)z^2_{\lambda_n}(a)+\frac{D_2}{2\lambda_n}kR^2\left(z'_{\lambda_n}(R)\right)^2\\&\quad+\frac{a^2k^2D_2}{2\lambda_n}\left(\frac{D_2}{D1}-\frac{1}{k}\right)\left(z'_{\lambda_n}(a)\right)^2\end{aligned}$$

$$= \frac{a^2(1-k)}{2}\begin{vmatrix} J_0\left(a\sqrt{\frac{\lambda_n}{D_2}}\right) & Y_0\left(a\sqrt{\frac{\lambda_n}{D_2}}\right) \\ J_0\left(R\sqrt{\frac{\lambda_n}{D_2}}\right) & Y_0\left(R\sqrt{\frac{\lambda_n}{D_2}}\right)\end{vmatrix}^2 + \frac{kR^2}{2}\begin{vmatrix} J_0\left(R\sqrt{\frac{\lambda_n}{D_2}}\right) & Y_0\left(R\sqrt{\frac{\lambda_n}{D_2}}\right) \\ J_1\left(R\sqrt{\frac{\lambda_n}{D_2}}\right) & Y_1\left(R\sqrt{\frac{\lambda_n}{D_2}}\right)\end{vmatrix}^2$$

$$+\frac{a^2k^2}{2}\left(\frac{D_2}{D1}-\frac{1}{k}\right)\begin{vmatrix} J_0\left(R\sqrt{\frac{\lambda_n}{D_2}}\right) & Y_0\left(R\sqrt{\frac{\lambda_n}{D_2}}\right) \\ J_1\left(a\sqrt{\frac{\lambda_n}{D_2}}\right) & Y_1\left(a\sqrt{\frac{\lambda_n}{D_2}}\right)\end{vmatrix}^2$$

where z_λ is defined in (4.30).

Proof We multiply (4.32) by rw'_{λ_n} to obtain

$$\begin{aligned} &\left[(rw'_{\lambda_n})^2\right]' + \tfrac{r^2\lambda_n}{D_1}[w^2_{\lambda_n}]' = 0, \quad 0 \le r < a \\ &\left[(rw'_{\lambda_n})^2\right]' + \tfrac{r^2\lambda_n}{D_2}[w^2_{\lambda_n}]' = 0, \quad a \le r < R. \end{aligned} \tag{4.34}$$

Integrating the first equation for $0 < r < a$ and second one for $a < r < R$ with respect to r, then applying integration by parts, we have

$$(aw'_{\lambda_n}(a-0))^2 + \frac{\lambda_n}{D_1}(aw_{\lambda_n}(a-0))^2 - \frac{2\lambda_n}{D_1}\int_0^a rw^2_{\lambda_n}(r)dr = 0 \tag{4.35}$$

$$(Rw'_{\lambda_n}(R))^2 - (aw'_{\lambda_n}(a+0))^2 - \frac{\lambda_n}{D_2}(aw_{\lambda_n}(a+0))^2 - \frac{2\lambda_n}{D_2}\int_a^R rw^2_{\lambda_n}(r)dr = 0.$$

According to (4.28), we have

$$\begin{aligned} D_1(aw'_{\lambda_n}(a-0))^2 - \frac{1}{k}D_2(aw'_{\lambda_n}(a+0))^2 &= D_1\left(a\frac{z_\lambda(a)}{y_\lambda(a)}y'_\lambda(a)\right)^2 - \frac{1}{k}D_2(akz'_\lambda(a))^2 \\ &= a^2k^2D_2\left(\frac{D_2}{D1}-\frac{1}{k}\right)\left(z'_{\lambda_n}(a)\right)^2. \end{aligned}$$

Thus, by multiplying the first equation by D_1 in (4.35) and the second one by D_2/k, respectively, and adding to the first one in (4.35), we obtain

$$\begin{aligned} \int_0^a rw^2_{\lambda_n}(r)dr + \frac{1}{k}\int_a^R rw^2_{\lambda_n}(r)dr &= \frac{1}{2}\left[(aw_{\lambda_n}(a-0))^2 - (aw_{\lambda_n}(a+0))^2\right] \\ &+ \frac{D_2}{2k\lambda_n}(Rw'_{\lambda_n}(R))^2 + \frac{a^2k^2D_2}{2\lambda_n}\left(\frac{D_2}{D1}-\frac{1}{k}\right)\left(z'_{\lambda_n}(a)\right)^2. \end{aligned}$$

According to the definition of w_λ given by (4.31), one can see that

$$w_{\lambda_n}(a-0) = z_{\lambda_n}(a), \quad w_{\lambda_n}(a+0) = kz_{\lambda_n}(a), \quad w_{\lambda_n}(R) = kz_{\lambda_n}(R)$$

which leads to the desired result.

The orthogonality relation allows us to compute the coefficients in the expansion of a piecewise smooth function $f(r) : 0 < r < R$, in a series of the form

$$f(r) = \sum_{n=1}^{\infty} A_n w_{\lambda_n}(r)$$

where $\{\lambda_n\}$ are the positive solutions of (4.28). To obtain $\{A_n\}$, we multiply the expansion by $w_{\lambda_n}(r)$ and integrate with respect to the weight rdr from 0 to R. This gives the formula

$$\begin{aligned} &\int_0^a f(r) r w_{\lambda_n}(r)dr + \frac{1}{k}\int_a^R f(r) r w_{\lambda_n}(r)dr \\ &\quad = A_n \left(\int_0^a r w_{\lambda_n}^2(r)dr + \frac{1}{k}\int_a^R r w_{\lambda_n}^2(r)dr \right) \end{aligned} \tag{4.36}$$

for $n = 1, 2, \ldots$. According to Lemmas 4.1 and 4.2, we have obtained:

Theorem 4.4 *Let f be a piecewise smooth function defined on* $[0, R]$. *Then the solution for the diffusion system* (2.6) *subject to edge conditions* (2.8) *and boundary condition* (2.7) *with a given initial condition $f(r)$ is given by*

$$u(r;t) = \sum_{n=1}^{\infty} A_n w_{\lambda_n}(r) e^{-(c_0+\lambda_n)t}$$

where $\{\lambda_n : n \geq 1\}$ are obtained from (4.28) *and $\{A_n : n \geq 1\}$ are defined by* (4.36).

Let us consider the case in which an individual insect is located at the origin $r = 0$. In such a case $f(r) = \frac{\delta(r)}{2\pi r}$. Then the solution $v(r;t)$ of (2.6)–(2.8) is the fundamental solution.

Corollary 4.5 *The fundamental solution for the diffusion system* (2.6) *subject to edge conditions* (2.8) *and boundary condition* (2.7) *is*

$$v(r;t) = \frac{1}{2\pi} \sum_{n=1}^{\infty} \frac{z_{\lambda_n}(a)}{\Delta_n y_{\lambda_n}(a)} w_{\lambda_n}(r) e^{-(c_0+\lambda_n)t}$$

where $\{\lambda_n : n \geq 1\}$ *are obtained from* (4.28) *and*

$$\Delta_n = \frac{a^2(1+k)}{2}\left|\begin{matrix} J_0\left(a\sqrt{\frac{\lambda_n}{D_2}}\right) & Y_0\left(a\sqrt{\frac{\lambda_n}{D_2}}\right) \\ J_0\left(R\sqrt{\frac{\lambda_n}{D_2}}\right) & Y_0\left(R\sqrt{\frac{\lambda_n}{D_2}}\right)\end{matrix}\right|^2 + \frac{kR^2}{2}\left|\begin{matrix} J_0\left(R\sqrt{\frac{\lambda_n}{D_2}}\right) & Y_0\left(R\sqrt{\frac{\lambda_n}{D_2}}\right) \\ J_1\left(R\sqrt{\frac{\lambda_n}{D_2}}\right) & Y_1\left(R\sqrt{\frac{\lambda_n}{D_2}}\right)\end{matrix}\right|^2$$

$$+\frac{a^2k^2}{2}\left(\frac{D_2}{D1}-\frac{1}{k}\right)\left|\begin{matrix} J_0\left(R\sqrt{\frac{\lambda_n}{D_2}}\right) & Y_0\left(R\sqrt{\frac{\lambda_n}{D_2}}\right) \\ J_1\left(a\sqrt{\frac{\lambda_n}{D_2}}\right) & Y_1\left(a\sqrt{\frac{\lambda_n}{D_2}}\right)\end{matrix}\right|^2. \tag{4.37}$$

5 Numerical simulations

We consider the case that insect has uniform density distribution in a disk inside Ω_a initially. Thus we let

$$f(r) = \begin{cases} M, & \text{if } \ 0 \leq r < a/2 \\ 0, & \text{if } \ a/2 \leq r \leq R \end{cases}$$

Then $A_n, n = 1, 2, \ldots$. can be obtained from

$$A_n = \frac{M\int_0^{a/2} rw_{\lambda_n}(r)dr}{\int_0^R rw_{\lambda_n}^2(r)dr} = \frac{aM\sqrt{D_1}z_{\lambda_n}(a)}{2\sqrt{\lambda_n}\Delta_n y_{\lambda_n}(a)} J_1\left(\frac{a}{2}\sqrt{\frac{\lambda_n}{D_1}}\right).$$

In simulations, we set $M = 10$, $D_1 = 1$, $D_2 = 2$, $a = 1$, and $R = 3$. We here demonstrate three cases: (i) $k_1 = 0.1, k_2 = 0.9$; (ii) $k_1 = k_2 = 0.5$; (iii) $k_1 = 0.9, k_2 = 0.1$ (Fig. 4).

Figure 5 shows that the probability distribution on $(0, a)$ has much higher density than the one on (a, R) due to the high return rate ($k_1 = 0.9$) of the insect upon encountering the edge $\partial\Omega_a$. When $k_1 = k_2 = 0.5$, the distribution on $(0, a)$ drops significantly as shown in Fig. 6. As the return rate continues to decrease ($k_1 = 0.1$), the distribution on $(0, a)$ drops further (Fig. 7). From these three cases, the distributions on (a, R) change only slightly comparing to those on $(0, a)$. The mean occupancy time on Ω_a and Ω_{R-a} are listed in Table 4, which shows that T_{Ω_a} is more sensitive than $T_{\Omega_{R-a}}$ with respect to the return rate k_1, in particular, when $k_1 >> k_2$. We also calculate the mean occupancy time for an individual located in the patch center initially (see Table 5).

6 Statistical properties

In this section, we briefly examine the statistical properties of these new estimators. The first step in this analysis is to determine the cumulative distribution function for occupancy time within a circle under various scenarios. We can then use this function to generate random variates with the appropriate distribution for occupancy time

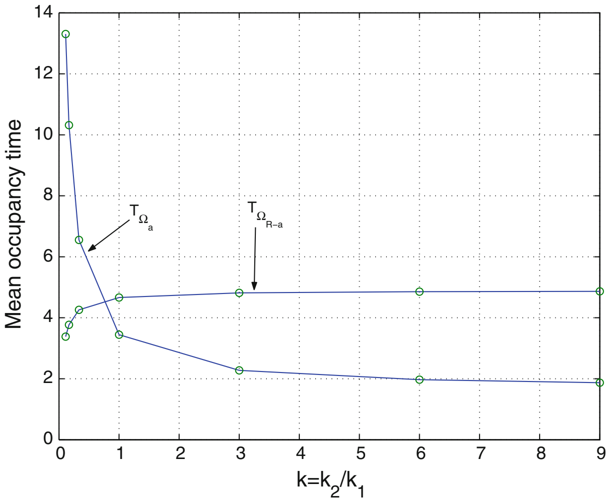

Fig. 4 Plot for mean occupancy time with $M = 10$, $c_0 = 0.2$

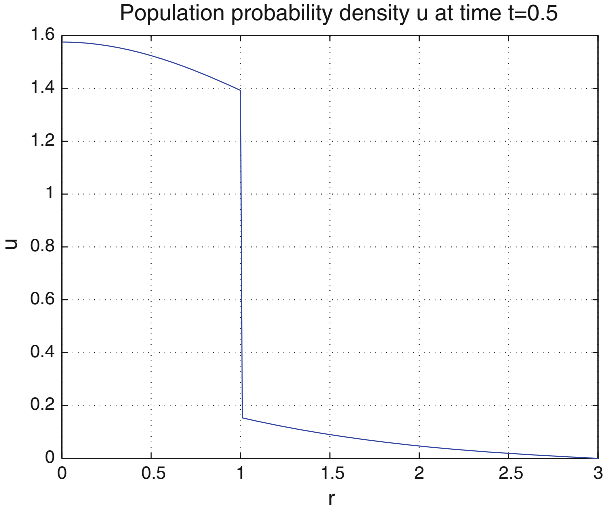

Fig. 5 Case 1: $t = 0.5$, $D_1 = 1$, $D_2 = 2$, $k_1 = 0.9$, $k_2 = 0.1$, $a = 1$, $R = 3$, and $c_0 = 0.2$. The truncation of the series is $N = 5$

using its inverse (Mood et al. 1974). We then examine the statistical behavior of our estimators using samples of these observations.

6.1 Cumulative distribution functions

Consider an insect initially located at $r = 0$ within a circle of radius a. The probability distribution $u(r, t)$ for its position at time t is given by (3.10). Using this distribution

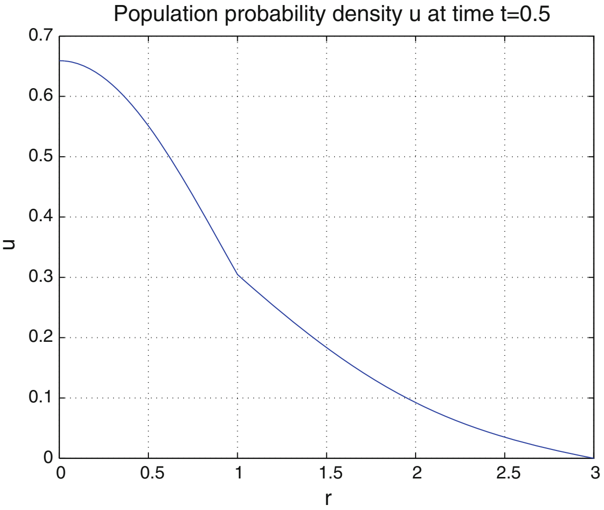

Fig. 6 Case 2: $t = 0.5$, $D_1 = 1$, $D_2 = 2$, $k_1 = k_2$, $a = 1$, $R = 3$, and $c_0 = 0.2$. The truncation of the series is $N = 5$

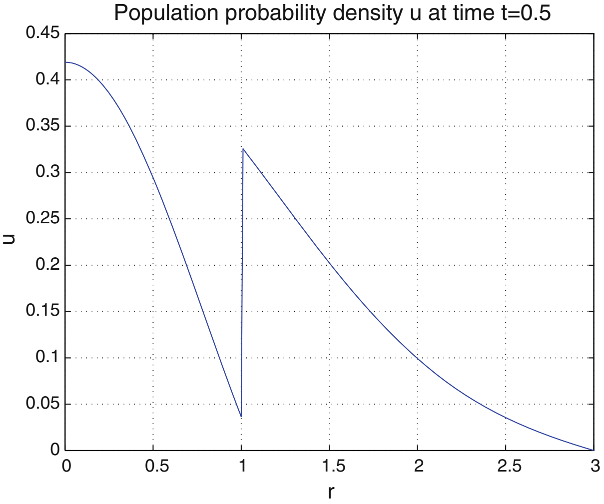

Fig. 7 Case 3: $t = 0.5$, $D_1 = 1$, $D_2 = 2$, $k_1 = 0.1$, $k_2 = 0.9$, $a = 1$, $R = 3$, and $c_0 = 0.2$. The truncation of the series is $N = 5$

Table 4 Mean occupancy time with uniform distribution initially, where $M = 10$, $c_0 = 0.2$

$k = k_2/k_1$	$k = 1/9$	$k = 1/6$	$k = 1/3$	$k = 1$	$k = 3$	$k = 6$	$k = 9$
$T\Omega_a$	13.3069	10.3184	6.5519	3.4456	2.2755	1.9697	1.8695
$T\Omega_{R-a}$	3.3809	3.7707	4.2610	4.6646	4.8160	4.8569	4.8671

Table 5 Mean occupancy time for individual located in the patch center initially

$k = k_2/k_1$	$k = 1/9$	$k = 1/6$	$k = 1/3$	$k = 1$	$k = 3$	$k = 6$	$k = 9$
T_{Ω_a}	1.7122	1.3334	0.8556	0.4607	0.3115	0.2724	0.2597
$T_{\Omega_{R-a}}$	0.4340	0.4847	0.5491	0.6035	0.6247	0.6306	0.6320

we can calculate the cumulative distribution function $F(t)$, which is defined as the probability the insect has dispersed from the circle or died inside the patch by time t. We have

$$\begin{aligned} F(t) &= 1 - \int_0^a 2\pi r u(r,t)dr \\ &= 1 - \int_0^a \sum_{n=1}^{\infty} \frac{2\pi r}{\pi a^2 J_1(\mu_n)} J_0(\frac{r}{a}\mu_n) e^{-(c_0 + D\mu_n^2/a^2)t} dr \\ &= 1 - \sum_{n=1}^{\infty} \frac{2}{a^2 J_1(\mu_n)^2} e^{-(c_0 + D\mu_n^2/a^2)t} \int_0^a r J_0(\frac{r}{a}\mu_n) dr \\ &= 1 - \sum_{n=1}^{\infty} \frac{2}{a^2 J_1(\mu_n)^2} e^{-(c_0 + D\mu_n^2/a^2)t} \frac{a^2}{\mu_n} J_1(\mu_n) \\ &= 1 - \sum_{n=1}^{\infty} \frac{2}{\mu_n J_1(\mu_n)} e^{-(c_0 + D\mu_n^2/a^2)t}. \end{aligned} \tag{6.38}$$

We can regard $F(t)$ as the cumulative distribution function for a random variable T, the occupancy time of the insect within the circle. Random variables with this distribution can be generated using the inverse of $F(t)$ and a source of uniform random variables. In particular, if U is a random variable with a uniform distribution on the interval (0, 1), then $T = F^{-1}(U)$ is a random variable with distribution function $F(t)$ (Mood et al. 1974). Because F^{-1} cannot be found explicitly, we generated random variates by numerically solving the equation $F(t) - u$ for t where u is a uniform random variate. We truncated the series for $F(t)$ at $n = 50$ terms in our simulations.

We can also calculate the mean occupancy time T_{Ω_a} for an insect released at $r = 0$ within a circle of radius a using previous results, obtaining

$$T_{\Omega_a} = 2a^2 \sum_{n=1}^{\infty} \frac{1}{J_1(\mu_n)\mu_n(c_0 a^2 + D\mu_n^2)}. \tag{6.39}$$

This result is used below to estimate D and c_0. It also provides a way of determining whether the random numbers generated using $F(t)$ have the appropriate mean.

We now consider an insect initially located at $r = 0$ within two concentric circles of radius a and R, with biased movement across the circle boundary at $r = a$, and different diffusion rates D_1 and D_2 for the two circles as well as mortality during dispersal at rate c_0. Suppose that k_1 describes the probability of an individual returning to Ω_a upon encountering the edge, while $k_2 = 1 - k_1$ is the probability of leaving Ω_a. Denote $k = k_2/k_1$. The probability distribution for its position at time t inside the disk $r \leq a$ is given by (see Corollary 4.5)

$$v(r;t) = \frac{1}{2\pi} \sum_{n=1}^{\infty} \frac{z_{\lambda_n}^2(a)}{\Delta_n y_{\lambda_n}^2(a)} y_{\lambda_n}(r) e^{-(c_0+\lambda_n)t}, \tag{6.40}$$

where y_{λ_n}, z_{λ_n} are defined in (3.19), and Δ_n by (4.37). Using this distribution, the probability that the insect has dispersed from the disk or died inside the patch is given by

$$\begin{aligned} G(t) &= 1 - \int_0^a 2\pi r v(r,t) dr \\ &= 1 - \sum_{n=1}^{\infty} \frac{z_{\lambda_n}^2(a)}{\Delta_n y_{\lambda_n}^2(a)} e^{-(c_0+\lambda_n)t} \int_0^a r y_{\lambda_n}(r) dr \\ &= 1 - a\sqrt{D_1} \sum_{n=1}^{\infty} \frac{z_{\lambda_n}^2(a)}{\Delta_n \sqrt{\lambda_n} y_{\lambda_n}^2(a)} J_1\left(a\sqrt{\frac{\lambda_n}{D_1}}\right) e^{-(c_0+\lambda_n)t} \end{aligned}$$

$G(t)$ can be regarded as the cumulative distribution function for a random variable T, defined as the occupancy time of an insect released within the circle of radius a. Random variates can also be generated using the same method as for $F(t)$ above. We truncated the series at $n = 50$ terms in our simulations.

The mean occupancy time for the disk $r \leq a$ is given by

$$T_{\Omega_a} = a\sqrt{D_1} \sum_{n=1}^{\infty} \frac{z_{\lambda_n}^2(a)}{\Delta_n \sqrt{\lambda_n}(c_0+\lambda_n) y_{\lambda_n}^2(a)} J_1\left(a\sqrt{\frac{\lambda_n}{D_1}}\right). \tag{6.41}$$

We will use this result below to estimate k.

6.2 Means, standard deviations, and confidence intervals

We used the above results to generate random samples for three scenarios. The first involves the dispersal of insects released at the center of a circle of radius $a = 1$, with no mortality during dispersal ($c_0 = 0$). We generated random samples of size $m = 100$ and 500 for known $D = 1$ using $F(t)$. These sample sizes are typical of the ones found in studies of insect dispersal (see Turchin 1998). For each sample, we then estimated D using the formula

Table 6 Mean and standard deviation of $\hat{D}$ for 1,000 random samples of occupancy time generated using $F(t)$, assuming $D = 1$, $c_0 = 0$, and a circle of radius $a = 1$

m	Mean $\hat{D}$	SD $\hat{D}$	% coverage (D)
100	1.004	0.070	93.6
500	1.000	0.030	94.5

Also listed is the percentage of 95 % confidence intervals obtained through bootstrapping that actually include D (% coverage)

$$\hat{D} = 0.2498 \frac{a^2}{\overline{T}}. \tag{6.42}$$

Here $\overline{T} = \frac{1}{m}\sum_{i=1}^{m} T_i$, where T_i is the ith occupancy time in the sample. This process was repeated 1,000 times, and the overall mean and standard deviation of $\hat{D}$ was calculated. Confidence intervals (95 %) were also calculated for each sample using bootstrapping and the percentile method (Manly 1997), and whether the interval included $D = 1$ noted. Our results suggest that $\hat{D}$ is an unbiased estimator of D, because its mean value lies close to D itself (Table 6). As would be expected, increased sample size reduce the variability of $\hat{D}$ because it decreases variability in $\overline{T}$. Confidence intervals obtained using bootstrapping had close to the correct coverage, containing D slightly less than 95 % of the time.

The second scenario involves the dispersal of insects released at the center of two circles, with radius $a = 1$ and $b = 2$, with mortality occurring during dispersal. We generated samples of occupancy times for each circle of size $m = 100$ and 500, setting $D = 1$ and $c_0 = 0.5$. The observations for each circle were separately generated and so were independent. We then estimated D and c_0 by numerically solving the two equations

$$\begin{aligned}\overline{T}_{\Omega_a} &= 2a^2 \sum_{n=1}^{\infty} \frac{1}{J_1(\mu_n)\mu_n(\hat{c}_0 a^2 + \hat{D}\mu_n^2)}\\ \overline{T}_{\Omega_b} &= 2b^2 \sum_{n=1}^{\infty} \frac{1}{J_1(\mu_n)\mu_n(\hat{c}_0 b^2 + \hat{D}\mu_n^2)}.\end{aligned}$$

Here $\overline{T}_a = \frac{1}{m}\sum_{i=1}^{m} T_{ai}$, where T_{ai} is the ith occupancy time for the circle of radius a, with $\overline{T}_{bi}$ similarly defined for second circle. We truncated the series in each equation at $n = 50$ terms. This process was repeated 1,000 times, and the overall mean and standard deviation of $\hat{D}$ and $\hat{c}_0$ was calculated. Bootstrap confidence intervals were also calculated for both parameters. The simulations suggest that $\hat{D}$ and $\hat{c}_0$ are unbiased estimates of D and c_0, while the bootstrap confidence intervals had coverage close to the nominal 95 % level (Table 7).

In the third scenario, an insect is released at $r = 0$ within two concentric circles of radius $a = 1$ and $R = 5$, with biased movement across the circle boundary at $r = a$. We are interested in estimating $k = k_2/k_1$, given that the other model

Table 7 Mean and standard deviation of $\hat{D}$ and $\hat{c}_0$ for 1,000 random samples of occupancy time generated using $F(t)$, assuming $D = 1$, $c_0 = 0.5$, and concentric circles of radius $a = 1$ and $b = 2$

m	Mean $\hat{D}$	SD $\hat{D}$	% coverage (D)	Mean $\hat{c}_0$	SD $\hat{c}_0$	% coverage (c_0)
100	1.007	0.107	94.7	0.495	0.220	94.0
500	1.000	0.048	94.5	0.503	0.098	94.8

Also listed is the percentage of 95 % confidence intervals obtained through bootstrapping that actually include D or c_0 (% coverage)

Table 8 Mean and standard deviation of $\hat{k}$ for 1,000 random samples of occupancy time generated using $G(t)$, assuming $D_1 = 1$, $D_2 = 2$, $c_0 = 0.5$, and concentric circles of radius $a = 1$ and $R = 5$

k	m	Mean $\hat{k}$	SD $\hat{k}$	% coverage (k)
0.2	100	0.211	0.057	94.5
0.2	500	0.202	0.022	94.6
0.5	100	0.533	0.147	92.2
0.5	500	0.506	0.059	94.9
1.0	100	1.113	0.386	92.9
1.0	500	1.022	0.143	92.9
2.0	100	2.444	1.630	90.5
2.0	500	2.074	0.408	94.5
5.0	100	7.441	5.538	90.8
5.0	500	5.612	2.098	93.0

Also listed is the percentage of 95 % confidence intervals obtained through bootstrapping that actually include k (% coverage)

parameters (D_1, D_2, and c_0) are known or estimated from prior studies. We generated samples of occupancy time ($m = 100$ or 500) for the inner circle using $G(t)$, setting $D_1 = 1$, $D_2 = 2$, and $c_0 = 0.5$, for $k = 0.2, 0.5, 1, 2$, and 5. We then used the method discussed in the text to find an estimate $\hat{k}$ using the sample mean $\overline{T}_a$ of occupancy times for the inner circle. We first generated values of the mean occupancy time T_{Ω_a} for a broad range of k values, ranging from $k = 0.05$ to $k = 20$. We then used piecewise cubic hermite interpolation to find $\hat{k}$ for the value of $\overline{T}_a$ for each sample. This process was repeated 1,000 times, and the overall mean and standard deviation found for $\hat{k}$ as well as bootstrap confidence intervals. For small values of k the estimates were close to the true parameter value, but for larger k there was increasing bias in the estimate (Table 8). The amount of bias was clearly less for the larger sample size, but the estimated values of k were always larger than the true parameter values. The confidence intervals had lower coverage than the nominal 95 % but were still adequate, with the lowest value being 90.5 %.

It is likely that the source of this bias is the nonlinear relationship between k and T_{Ω_a} combined with the fact that $\overline{T}$ is a random variable. Let g be the function describing the relationship k and T_{Ω_a}. Our method essentially uses $\hat{k} = g(\overline{T})$ to estimate k. By Jensen's inequality, we have $E[\hat{k}] = E[g(\overline{T})] \geq g(E[\overline{T}]) = g(T_{\Omega_a})$ because g is a convex function (Mood et al. 1974). We would therefore expect the estimated values of k to exceed the true parameter values, which is the pattern observed in Table 8. The amount of bias decreases with sample size because $\overline{T}$ is less variable under these circumstances.

7 Concluding remarks

In this paper, we present a new approach for the estimation of the diffusion rate as well as the crossing probability for one type of edge behavior, a biased random walk. The system is not a classical diffusion system and the dynamical behaviors are coupled at the interface boundaries, which present mathematical challenges in seeking solutions, either analytical expressions or numerical computational schemes. We studied the solvability of the diffusion system using Bessel functions and obtain mathematical expressions for the mean occupancy times and conditional probability densities across different types of habitat.

The expression obtained for the diffusion rate D given by (2.3) has two major advantages over the traditional maximum likelihood approach. The first is that occupancy time is not a difficult quantity to be measured (see below). The second is that the proposed approach has a low computational cost. These two features make the approach quite attractive. Furthermore, notice that the method allows us to choose a relatively small patch, so that even if a nonlinear term appears in the diffusion process (such as in Fisher PDE model, Kolmogorov et al. 1991) we can still use a linear model to approximate it, and thus use (2.3) for estimation.

The crossing probability for biased edge movement between two different habitat types usually is difficult to obtain since the model in such a case is no longer a standard diffusion model, and the currently used maximum likelihood approach is computationally intensive. The mathematical expressions for the mean occupancy time given by (3.15) and (3.17) allow us to compute a set of mean occupancy times by preselecting a set of values $k = k_2/k_1$ with $k_1 + k_2 = 1$. Then the ratio $k = k_2/k_1$ can be estimated by piecewise cubic Hermite interpolation. The accuracy can be improved by simply increasing the size of the preselected set appropriately. This approach is mainly to avoid to solve a highly nonlinear equation to obtain k under our framework.

Our analyses using simulated data sets suggests these new estimation methods yield unbiased estimates of the diffusion rate as well as mortality during dispersal. Confidence intervals for these estimates can also be obtained through bootstrapping. We did observe some bias in the estimation of the $k = k_2/k_1$, which was greatest for large values of this parameter and small data sets. Large values of k would seem unlikely in nature, because they imply the insects would flee a patch of habitat upon reaching the edge.

Mean occupancy time can be estimated in a number of ways through field experiments or observations. We first suppose that mortality during dispersal is negligible, either because it is truly low, or the circular region under consideration is sufficiently small that the insects are unlikely to die before they exit. To estimate the mean occupancy time, we need only observe when a number of insects or organisms leave a circular region, and take the average of these values. Such data might be obtained by releasing the insects within the circle, or we may be able to initially locate an insect and then determine when it leaves a circle surrounding the initial position. The insects could be directly observed leaving the circle, or traps deployed that indicate the direction of insect movement. For example, a common type of insect trap is a flat panel coated with a sticky substance, and these could be deployed facing inward at the edge of the circle. Insects trapped on the inward side of the trap would be considered to have left the circle. The traps would be checked at regular intervals and the time of arrival (the occupancy time) recorded for each insect. We would then use (2.4) and the average of these occupancy times to obtain an estimate of D, and bootstrapping to obtain a confidence interval.

We next suppose there is significant mortality during dispersal, and that one can determine when an insect dies as well as exits the circle. The mean occupancy time can still be calculated in this case, but now includes the time of death for some individuals, in particular those that die before exiting the circle. One would then observed the occupancy times for insects for two circles of different radius, and solve for D and the mortality rate c_0 using (2.5). These extra observations and calculations may be avoidable in some systems by choosing a sufficiently small circle that mortality is negligible during the course of the experiment, because most insects would exit the circle before dying. Once we have estimated the diffusion rates for different types of habitat or matrix (D_1 and D_2) and any mortality (c_0), we would then apply the same experimental protocols to estimate the boundary parameter k_1. Insects would be released within a circle of habitat, and the time when they leave the circle as well as the time of death recorded. We would then estimate the edge crossing probability k_1 using the methods in Sect. 2.2, which make use of the relationship between k_1 and mean occupancy time. We are currently developing software programs that automate these calculations, and applying them to real data sets, to make these procedures more practical and useful to field ecologists.

References

Cain ML (1990) Models of clonal growth in Solidago altissima. J Ecol 78:27–46

Cantrell RS, Cosner C (2003) Spatial ecology via reaction–diffusion equations. Wiley, Chichester

Cronin JT (2007) From population sources to sieves: the matrix alters host-parasitoid source-sink structure. Ecology 88:2966–2976

Cronin JT, Haynes KJ (2004) An invasive plant promotes unstable host-parasitoid patch dynamics. Ecology 85:2772–2782

Cronin JT, Reeve JD, Wilkens R, Turchin P (2000) The pattern and range of movement of a checkered-beetle predator relative to its bark-beetle prey. Oikos 90:127–138

Fagan WF (1997) Introducing a "boundary-flux" approach to quantifying insect diffusion rates. Ecology 78:579–587

Haynes KJ, Cronin JT (2003) Matrix composition affects the spatial ecology of a prairie planthopper. Ecology 84:2856–2866

Haynes KJ, Cronin JT (2006) Interpatch movement and edge effects: the role of behavioral responses to the landscape matrix. Oikos 113:43–54

Kareiva P, Odell G (1987) Swarms of predators exhibit "preytaxis" if individual predators use area-restricted search. Am Nat 130:233–270

Kolmogorov A, Petrovskii I, Piscounov N (1991) A study of the diffusion equation with increase in the amount of substance, and its application to a biological problem. In: Tikhomirov VM (ed) Selected Works of A. N. Kolmogorov I. Kluwer, Dordrecht, pp 248–270

Lawrence WS, Bach CE (1989) Chrysomelid beetle movements in relation to host-plant size and surrounding non-host vegetation. Ecology 70:1679–1690

Manly BFJ (1997) Randomization, bootstrap and Monte Carlo methods in biology. Chapman & Hall, New York

Min A, Cronin JT, Reeve JD, Xiao M, Xu D (2012) Identification of diffusion coefficient and returning probability in nonhomogeneous landscapes (preprint)

Mood AM, Graybill FA, Boes DC (1974) Introduction to the theory of statistics, 3rd edn. McGraw-Hill, New York

Okubo A, Levin SA (2001) Diffusion and ecological problems: modern perspectives, 2nd edn. Springer, New York

Ovaskainen O (2004) Habitat-specific movement parameters estimated using mark-recapture data and a diffusion model. Ecology 85:242–257

Ovaskainen O, Cornell SJ (2003) Biased movement at a boundary and conditional occupancy times for diffusion processes. J Appl Probab 40:557–580

Pinsky MA (1998) Partial differential equations and boundary-value problems with applications. American Mathematical Society, Providence

Reeve JD, Haynes KJ, Cronin JT (2008) Diffusion models for herbivore movement incorporating heterogeneity among substrates, individuals and edge behaviors. J Anim Ecol 77:898–904

Reeve JD, Cronin JT (2010) Edge behavior in a minute parasitic wasp. J Anim Ecol 79:483–490

Ricketts TH (2001) The matrix matters: effective isolation in fragmented landscapes. Am Nat 158:87–99

Ries L, Debinski DM (2001) Butterfly responses to habitat edges in highly fragmented prairies of central Iowa. J Anim Ecol 70:840–852

Roland J, Keyghobadi N, Fownes S (2000) Alpine Parnassius butterfly dispersal: effects of landscape and population size. Ecology 81:1642–1653

Sharon E, Mumford D (2007) 2D-shape analysis using conformal mapping. Int J Comput Vis 70(1):55–75

Turchin P (1998) Quantitative analysis of movement: measuring and modeling population redistribution in plants and animals. Sinauer Associates, Sunderland